

## SPECIFIC CONTACT RESISTANCE OF METAL-SEMICONDUCTOR BARRIERS

C. Y. CHANG, Y. K. FANG

College of Engineering, National Chiao Tung University, Hsinchu, Taiwan, Republic of China

and

S. M. SZE

Bell Telephone Laboratories, Incorporated, Murray Hill, New Jersey 07974 U.S.A.

(Received 22 September 1970; in revised form 10 December 1970)

**Abstract**—The specific contact resistance at zero bias,  $R_c$ , serves as a measure of the ohmic or rectifying behavior of a metal-semiconductor barrier under operating conditions. It is thus an important design parameter for semiconductor devices. The values of  $R_c$  have been calculated for Metal-Si and metal-GaAs barriers on  $p$ -type and  $n$ -type samples. The theoretical calculation is based on the generalized transport study of metal-semiconductor systems.

The results, which are presented graphically, show the dependence of  $R_c$  on temperature over the range 50°K–500°K, the barrier height from 0.2 to 1.0 eV, and the ionized impurity concentration from  $10^{14}$  to  $10^{21}$  cm<sup>-3</sup>. Generally  $R_c$  decreases exponentially with increasing temperature and with decreasing barrier height. For samples with lower dopings where the thermionic emission dominates,  $R_c$  is essentially independent of doping; for higher dopings where the tunneling dominates,  $R_c$  decreases rapidly with increasing doping. The experimental results of  $R_c$  for various metals on silicon samples are in good agreement with the predictions.

**Resumé**—La résistance de contact spécifique à polarisation nulle,  $R_c$ , sert de mesure du comportement ohmique ou de redressement d'une barrière métal-semiconducteur dans des conditions de fonctionnement. Il est ainsi important en tant que paramètre de conception pour les dispositifs semi conducteurs. Les valeurs de  $R_c$  ont été calculées pour les barrières métal-Si et métal-GaAs sur des échantillons du type  $-p$  et du type  $-n$ . Le calcul théorique est fondé sur l'étude de transport généralisé de systèmes métal-semiconducteurs.

Les résultats, présentés graphiquement, montrent la dépendance de  $R_c$  sur la température dans la gamme de 50°K à 500°K, la hauteur de barrière entre 0.2 et 1.0 eV, et la concentration d'impureté ionisée entre  $10^{14}$  et  $10^{21}$  cm<sup>-3</sup>. Généralement  $R_c$  diminue exponentiellement avec l'accroissement de température et avec le décroissement de la hauteur de barrière. Pour les échantillons avec doping plus faible où l'émission thermoionique domine,  $R_c$  est essentiellement indépendant du doping; pour un doping plus élevé où le tunnellement domine,  $R_c$  décroît rapidement à mesure que le doping augmente. Les résultats expérimentaux de  $R_c$  pour divers échantillons de métal sur silicium sont en bon accord avec les prévisions.

**Zusammenfassung**—Bei einem Halbleiter-Metall-Kontakt unter Betriebsbedingungen dient der spezifische Kontaktwiderstand  $R_c$  ohne Vorspannung als Maß für ohmsches Verhalten oder Gleichrichterwirkung. Er ist daher eine wichtige Größe bei der Konstruktion von Halbleiterbauelementen. Die Werte für  $R_c$  wurden für Metall-Silizium- und Metall-Galliumarsenid-Barrieren mit  $p$ - oder  $n$ -Typ Kristallen berechnet. Die theoretische Rechnung beruht auf einer verallgemeinerten Studie der Transporteigenschaften eines Metall-Halbleiter-Systems.

Die graphisch wiedergegebenen Ergebnisse zeigen den Verlauf von  $R_c$  für einen Temperaturbereich von 50°K bis 500°K, Barrierenhöhen zwischen 0.2 und 1.0 eV und Konzentrationswerte der ionisierten Störstellen von  $10^{14}$ /cm<sup>3</sup> bis  $10^{21}$ /cm<sup>-3</sup>. Ganz allgemein nimmt  $R_c$  mit der Temperatur ab und mit der Barrierenhöhe zu. Bei Proben mit niedrigerer Dotierung, wo die thermische Emission überwiegt, ist  $R_c$  im wesentlichen von der Konzentration unabhängig. Mit höherer Dotierung nimmt  $R_c$  rasch wegen des überwiegenden Tunnelstromes ab. Die experimentellen Ergebnisse für  $R_c$  mit verschiedenen Metallen auf Silizium sind in guter Übereinstimmung mit den vorhergesagten Werten.

### 1. INTRODUCTION

THE SPECIFIC contact resistance is defined as the reciprocal of the derivative of current density with respect to voltage. When evaluated at zero bias, this specific contact resistance,  $R_c$ , is an important figure of merit for the transport characteristic of a metal–semiconductor barrier. For example, for a good ohmic contact, [1] it is required that the value of  $R_c$  should be sufficiently small so that the observed linear current–voltage characteristic is mainly due to the series resistance of the semiconductor material near the contact.

Based on the generalized majority-carrier transport theory [2], we shall obtain the specific contact resistance for metal–Si and metal–GaAs barriers on  $p$ -type and  $n$ -type samples. For a given semiconductor, the value of  $R_c$  depends on the temperature, the barrier height, and the impurity concentration. We shall present in graphical form the values of  $R_c$  over practical ranges of these parameters. These results are useful in designing and characterizing many semiconductor devices operated at various current and temperature ranges.

The basic transport equation of a metal–semiconductor system is presented in Section 2. The expressions for the specific contact resistance and its thermal coefficient are derived in Section 3; while the computed results are given in Section 4. A summary is presented in Section 5.

### 2. BASIC TRANSPORT EQUATION

The energy band diagram of a metal–semiconductor barrier under equilibrium conditions is shown in Fig. 1 where  $\Delta\phi$  is the barrier lowering due to image force,  $\phi_B$  is the barrier height, and  $V_{bo}$  is the built-in potential. The energy  $\xi$  is measured upward from the barrier maximum which is used as a reference, while  $\eta$  is measured downward from the reference. (Both  $\Delta\phi$  and  $\phi_B$  are dependent on the applied voltage.)

The basic transport equation in a metal–semiconductor barrier is given by [2]

$$J = J_{SM} - J_{MS} \quad (1)$$

where  $J$  is the total current density,  $J_{SM}$  is the current density flowing from the semiconductor to the metal, and  $J_{MS}$  is the corresponding current density flowing from the metal to the semiconductor.

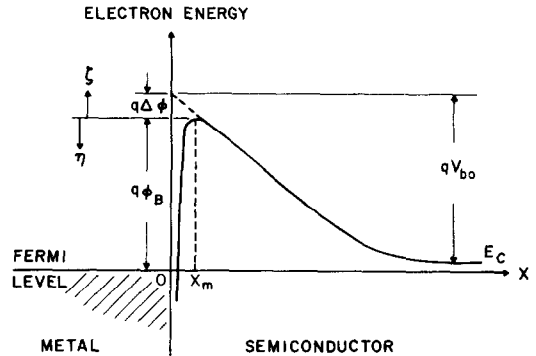


Fig. 1. Energy band diagram of a metal–semiconductor contact at thermal equilibrium.

The expression for  $J_{SM}$  at a bias voltage  $V$  is given by

$$J_{SM}(V) = \frac{A^*T}{k} \int_0^\infty P(\xi) e^{-(q\phi_B - qV + \xi)/kT} d\xi + \frac{A^*T}{k} \int_0^{(qV_{bo} - V - \Delta\phi)} F_S P(\eta) (1 - F_m) d\eta \quad (2)$$

where  $A^*$  is the effective Richardson constant, and  $F_S$  and  $F_m$  are the Fermi–Dirac distribution functions in the semiconductor and in the metal respectively.  $P(\xi)$  and  $P(\eta)$  are the quantum transmission functions above and below the barrier maximum respectively. The first term on the right-hand of equation (2) represents the contribution from thermionic emission of carriers over the barrier maximum. The second term is the tunneling component. The expression for the other current density  $J_{MS}$  is essentially the same as that given by equation (2) except that the exponential term is replaced by  $\exp[-(q\phi_B + \xi)/kT]$ . The relative magnitude of the thermionic emission and tunneling components depends on the barrier height, temperature, and doping concentration which is implicit in the transmission functions. For degenerate semiconductors, the product of distribution functions,  $F_S(1 - F_m)$  in equation (2) is replaced [3] by  $\ln\{1 + \exp[(E - E_F)/kT]\}$ , where  $E_F$  is the Fermi level.

### 3. SPECIFIC CONTACT RESISTANCE

As mentioned previously, the specific contact

resistance is defined as

$$R_c \equiv \left( \frac{\partial J}{\partial V} \right)_{V=0}^{-1}. \quad (3)$$

Since the accurate quantum transmission functions have to be obtained by numerical analysis, it is difficult to express  $J$  and  $R_c$  in closed forms. We shall, however, consider two limiting cases so that a clear physical picture can be obtained for  $R_c$ . The exact calculations of  $R_c$  will be presented in Section 4.

3.1. *Thermionic emission.* For samples of lower doping concentrations the thermionic-emission component dominates the current transport so that the second term in equation (2) can be neglected. If we assume that the transmission function is unity, we can obtain the standard Richardson expression for the current density  $J_{SM}$ :

$$J_{SM} = J_s e^{qV/kT} \quad (4)$$

where  $J_s$  is the saturation current density given by

$$J_s = A^* T^2 e^{-q\phi_B/kT}. \quad (4a)$$

The total current density is then

$$J = J_{SM} - J_{MS} = J_s (e^{qV/kT} - 1). \quad (5)$$

From equations (3), (4a) and (5), the specific contact resistance is given as

$$R_c = \frac{k}{qA^*T} e^{q\phi_B/kT} = \frac{kT}{qJ_s}. \quad (6)$$

In deriving equation (6) we have neglected the small voltage dependence of the barrier height.

The thermal coefficient of  $R_c$  is defined as

$$\gamma \equiv -\frac{1}{R_c} \frac{\partial R_c}{\partial T} = (1 + q\phi_B/kT)/T. \quad (7)$$

It is clear from equation (6) that  $R_c$  will decrease exponentially with increasing temperature and with decreasing barrier height. The value of  $R_c$  will be inversely proportional to the effective Richardson constant; this means that  $R_c$  will decrease with increasing effective mass for the cases where the thermionic emission dominates. From equation (7) we note that the thermal coef-

ficient will also decrease with increasing temperature and with decreasing barrier height.

3.2. *Tunneling.* For samples of higher doping concentrations, the tunneling process may dominate, and we can neglect the first term in equation (2). If we use the WKB approximation for the transmission function we obtain [3, 4]

$$P(\eta) = \exp [-q(V_{b0} - V)/E_{00}] \quad (8)$$

where

$$E_{00} = \frac{\hbar}{2} \sqrt{\left( \frac{N}{\epsilon_s m^*} \right)}.$$

The quantity  $E_{00}$  is a reference energy which depends on the doping  $N$ , the semiconductor permittivity  $\epsilon_s$ , and the effective mass  $m^*$ .

Substitution of equation (8) into equations (2) and (3) yields

$$R_c \sim \left( \frac{1}{E_{00}} \right) \exp (qV_{b0}/E_{00}). \quad (9)$$

From equation (9) it is clear that in the tunneling range the specific contact resistance is independent of temperature (or  $\gamma \ll 1$ ). Equation (9) indicates that for the tunneling case,  $R_c$  depends strongly on the the doping concentration and the tunneling effective mass, and decreases exponentially with the factor  $\sqrt{(N/m^*)}$ .

#### 4. RESULTS

To calculate the specific contact resistance,  $R_c$ , and its thermal coefficient,  $\gamma$ , we use the pertinent Richardson constant [5]  $A^*$ , the tunneling effective mass, [6] and the dynamic dielectric constant [7] corresponding to the carrier transit time from the metal-semiconductor interface to the potential maximum (from  $x = 0$  to  $x = x_m$  as shown in Fig. 1). Table 1 lists the room-temperature values of the effective Richardson constants and dielectric constants for various silicon and GaAs metal-semiconductor systems.

In silicon the tunneling effective mass which is a strong function of temperature and doping concentration, can be expressed as

$$m^* = [l^2/m_t + (m^2 + n^2)/\sqrt{(m_d^3/m_t)}]^{-1} \quad (10)$$

where  $l$ ,  $m$ , and  $n$  are the directional cosines of carrier transport with respect to the main axis of

Table 1. Effective Richardson constant and dielectric constant at 300°K

Semiconductor	Type	Orientation	$A^*$ (amp/cm <sup>2</sup> °K)	$\epsilon_s/\epsilon_0$
Si	<i>n</i>	$\langle 111 \rangle$	270	12
		$\langle 100 \rangle$	200	
	<i>p</i>	—	79	
GaAs	<i>n</i>	—	8	11
	<i>p</i>	—	74	

one valley,  $m_l$  is the longitudinal effective mass, and  $m_d$  is the density of state effective mass. From the measured results [6, 8] of  $m_d$  and  $m_l$ , the value of the tunneling effective mass can be determined from equation (10) and is shown in Fig. 2 as a function of temperature and doping concentration for *n*-type,  $\langle 111 \rangle$  oriented silicon. For dopings lower than  $5 \times 10^{17}$  cm<sup>-3</sup>, the mass  $m^*$  is essentially the same as that of  $5 \times 10^{17}$  cm<sup>-3</sup>. For higher dopings, however,  $m^*$  increases with the doping.

For GaAs the dependence of the tunneling effective mass on temperature and doping concentration is still under investigation [9], we shall assume that the tunneling effective mass has its low-temperature value, i.e.  $0.068 m_0$  for electrons and  $0.12 m_0$  for holes where  $m_0$  is the free electron mass.

Figure 3 shows the theoretical  $R_c$  at room temperature for *n*-type (solid lines) and *p*-type (dotted lines),  $\langle 111 \rangle$ -oriented silicon samples of various doping concentrations and barrier heights. For a given doping concentration,  $R_c$  decreases with decreasing  $\varphi_B$ ; and for a given  $\varphi_B$ ,  $R_c$  decreases with increasing  $N$ . These results are consistent with equations (6) and (9). Also shown in Fig. 3 are some experimental results of Al-Si ( $\varphi_B \approx 0.6$  V), [10] Mo-Si ( $\varphi_B \approx 0.6$  V), [10] and PtSi-Si ( $\varphi_B = 0.85$  V) [2] barriers. It is apparent that the agreement between theory and experiment is reasonably good. Similar results for GaAs samples are shown in Fig. 4. The general features are the same as Fig. 3. However, in the tunneling range,  $R_c$  for GaAs is smaller because of its smaller effective mass.

From these figures, it is clear that to obtain a given  $R_c$  (e.g. for a contact of  $10^{-4}$  Ω-cm<sup>2</sup> in silicon) we can either use a heavily doped sample with a relatively high barrier height (say  $N = 4 \times 10^{19}$  cm<sup>-3</sup>

for  $\varphi_B = 0.8$  V) or a lightly doped sample with a lower barrier height (say  $N = 3 \times 10^{18}$  cm<sup>-3</sup> for  $\varphi_B = 0.4$  V). Table 2 lists some values of  $R_c$  for PtSi-Si contacts formed on  $\langle 111 \rangle$  oriented *n*-type silicon.

Table 2.  $R_c$  for PtSi-Si contacts ( $\varphi_B = 0.85$  V) on  $\langle 111 \rangle$  oriented *n*-type silicon

$R_c$ (Ω-cm <sup>2</sup> ) $N_D$ (cm <sup>-3</sup> )	$T$		
	200°K	300°K	400°K
$10^{16}$	$5 \times 10^{11}$	$2 \times 10^5$	20
$10^{17}$	$2 \times 10^{11}$	$10^5$	10
$10^{18}$	$2 \times 10^9$	$10^4$	6
$10^{19}$	10	1	0.5
$10^{20}$	$10^{-5}$	$10^{-5}$	$2 \times 10^{-5}$

The results of temperature dependence of  $R_c$  for various samples are shown in Figs. 5–8 where the doping concentration and barrier height are used as parameters. We note that in the thermionic emission range ( $10^{14} \sim 10^{17}$  cm<sup>-3</sup>),  $R_c$  is essentially independent of doping concentration. This is consistent with equation (6). In the tunneling range ( $>10^{18}$  cm<sup>-3</sup>), however,  $R_c$  becomes a strong function of doping. It is also interesting to note that a good rectifying contact (large  $R_c$ ) at lower temperatures may become a good ohmic contact (small  $R_c$ ) when the operating temperature is increased. Hence, for high-power elevated-temperature operation, the high-temperature values of  $R_c$  should be used in the device design theory.

The thermal coefficients of  $R_c$  are shown in Figs. 9 and 10 for *n*-type silicon and *n*-type GaAs respectively. Similar results can be obtained for *p*-type samples. We note that the general feature

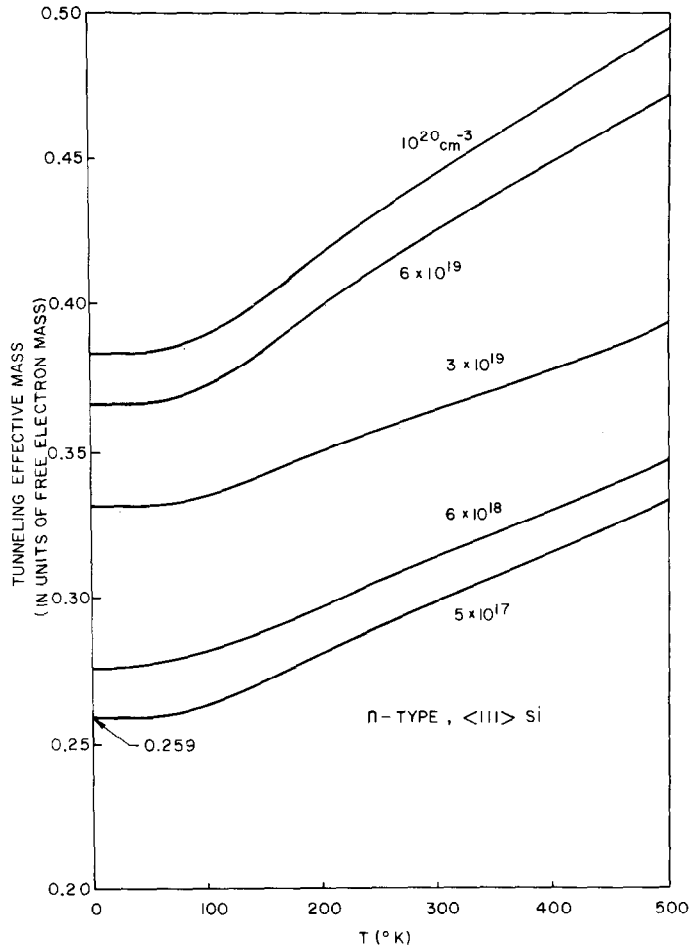


Fig. 2. Tunneling effective mass as a function of temperature and doping concentration for *n*-type, (111) oriented silicon.

of the temperature dependence of  $\gamma$  follows equation (7), i.e.  $\gamma$  decreases with decreasing  $\phi_B$  and increasing  $T$ . To obtain low thermal coefficient of  $R_c$ , we should use samples of low barrier height and large doping concentration. For Si samples,  $\gamma$  changes sign at  $3 \times 10^{19} \text{ cm}^{-3}$ , causing a discontinuity in  $\ln \gamma$  as shown in Fig. 9. This is mainly due to the effect of the tunneling effective mass which increases with doping as shown in Fig. 2.

5. SUMMARY

The dependence of the specific contact resistance,  $R_c$ , on various parameters can be summarized as follows:

(1) Ionized impurity concentration: As the concentration increases, the depletion width becomes narrower, which in turn causes the transmission coefficient for tunneling to increase. Thus, even a high barrier contact can become ohmic if the barrier is thin enough such that tunneling dominates the carrier transport process (as can be seen in Figs. 3 and 4). Because of the statistical nature of impurity distribution in the samples, as the impurity concentration increases, it is expected that the saturation current density will become larger than the value calculated for the average concentration[2]. This in turn will cause some reduction of  $R_c$ .

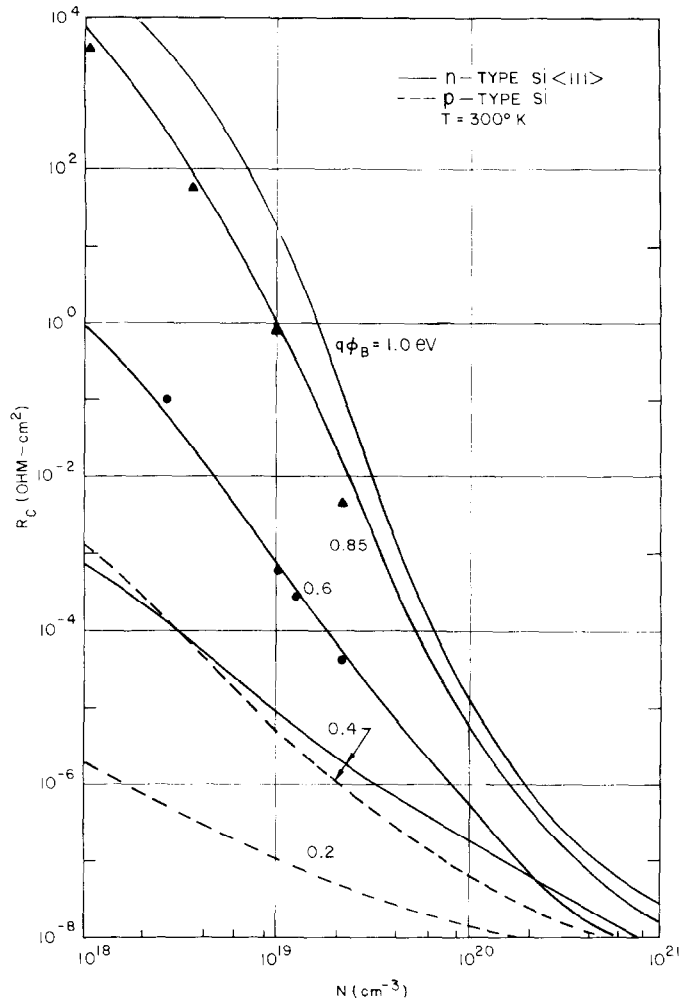


Fig. 3. Theoretical specific contact resistance at 300°K for *n*-type,  $\langle 111 \rangle$  oriented (solid lines) and *p* type (dotted lines) silicon. The solid circles are experimental results of Al-Si and Mo-Si barriers ( $q\phi_B = 0.6$  eV), and triangles for PtSi-Si barriers ( $q\phi_B = 0.85$  eV).

(2) Temperature: The temperature effect arises from the distribution functions. For higher temperatures more carriers are excited above the Fermi level. The current density is increased, causing a decrease in  $R_c$  as shown in Figs. 5–8.

(3) Barrier height: As the barrier height decreases, both the thermionic emission component and the transmission coefficient increase. There is a large number of carriers which can transport from the semiconductor band edges to the metal

and vice versa. The contact resistance will be low. However, as the doping increases, the barrier height will become less important (referring to Figs. 3 and 4 where all curves converge at high doping limits).

(4) Effective Richardson constant: This constant generally depends on the crystal orientation (e.g. for Si) and can modulate the magnitude of the carrier transport mechanism. In the high temperature region, the phonon scattering effect [11]

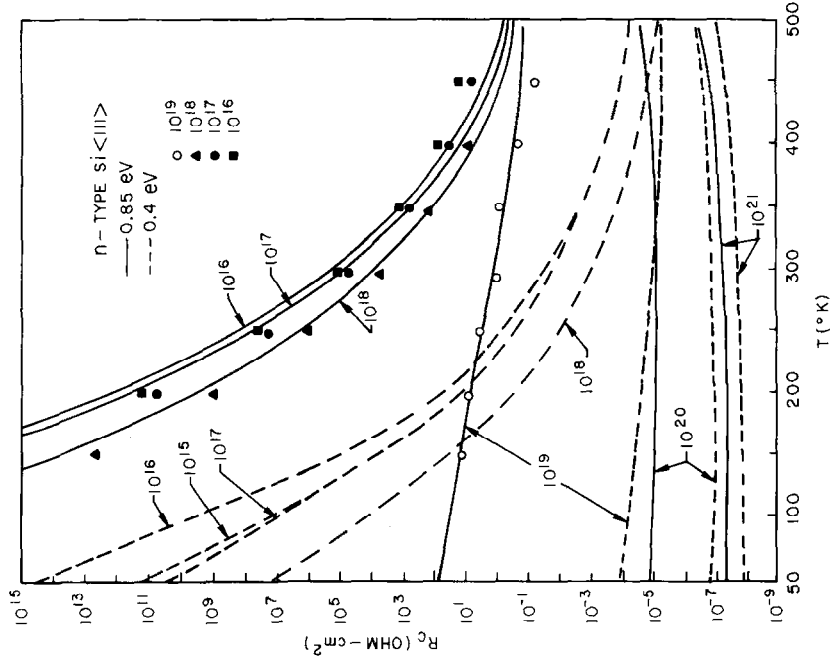


Fig. 5. Specific contact resistance for n-type (111) Si samples vs. temperature. Barrier height and doping concentration are parameters. Also shown are experimental results of PtSi-Si barriers made on silicon substrates of various dopings.

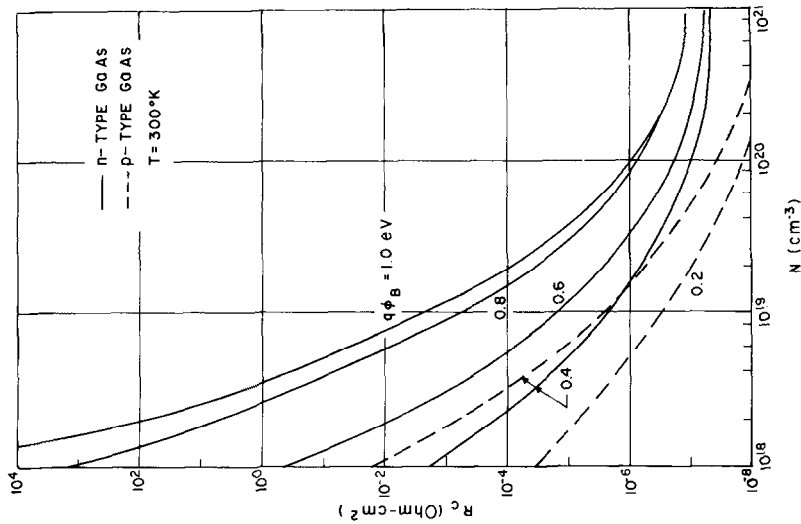


Fig. 4. Specific contact resistance at  $300^{\circ}\text{K}$  for  $n$ -type and  $p$ -type GaAs.

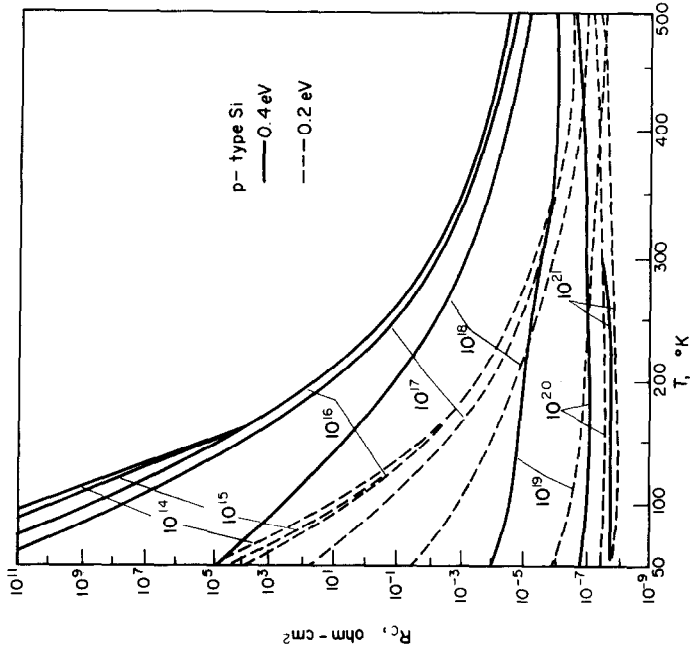


Fig. 7. Specific contact resistance for p-type Si samples.

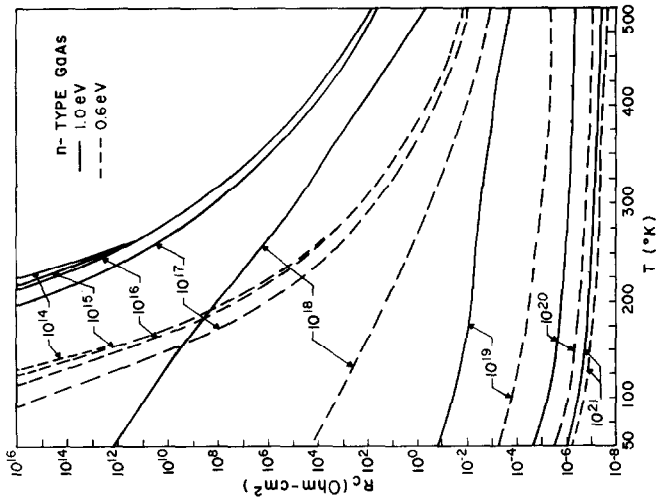


Fig. 6. Specific contact resistance for n-type GaAs samples vs. temperature. Barrier height and doping are parameters.

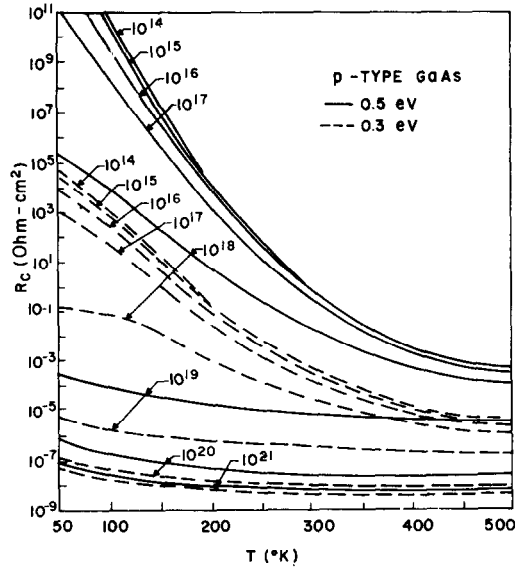


Fig. 8. Specific contact resistance for *p*-type GaAs samples.

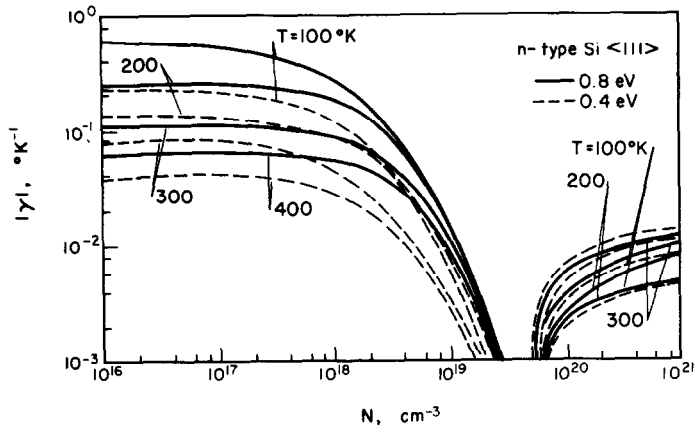


Fig. 9. Thermal coefficient vs. doping concentration for *n*-type,  $\langle 111 \rangle$  Si samples.

will slightly reduce the value of  $A^*$ . However,  $A^*$  has relatively small effect on  $R_c$  in comparison with the barrier height or the impurity concentration.

(5) Tunneling effective mass: Small effective mass will give rise to large transmission coefficient. small values of  $R_c$  can be obtained for materials with small tunneling effective mass. The mass depends upon the direction of carrier transport if

the band extrema do not occur at the center of the Brillouin zone and when the constant energy surface is not spherical. For *n*-type Si in the  $\langle 100 \rangle$  direction the low-temperature tunneling effective mass is  $0.1905 m_0$  which is smaller than that for  $\langle 111 \rangle$ -oriented samples. The values of  $R_c$  for *n*-type  $\langle 100 \rangle$ -oriented Si are about a factor of two lower than that shown in Fig. 3. For a given doping,

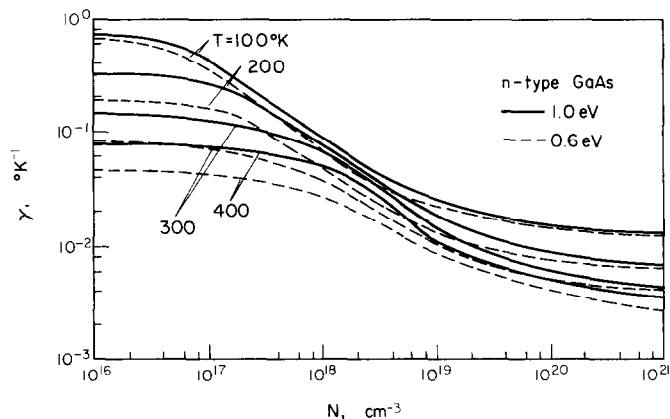


Fig. 10. Thermal coefficient vs. doping concentration for *n*-type GaAs samples.

the tunneling effective mass is a function of temperature. This may cause the specific contact resistance to increase slightly at higher temperatures (e.g. for dopings of  $10^{20}$  and  $10^{21}$   $\text{cm}^{-3}$  in Figs. 5 and 7).

The results of  $R_c$  which are presented in Figs. 3–8 cover the practical ranges of temperature, doping, and barrier height. These results are believed to be useful in design theory of many semiconductor devices.

*Acknowledgement*—We wish to thank Prof. L. J. Chu and Dr. R. M. Ryder for many helpful discussions and suggestions. The assistance of computation work by the computer Center, Engineering Science Research Center, National Science Council is deeply appreciated.

#### REFERENCES

1. For a general review see B. Schwartz, *Ohmic Contacts to Semiconductors* Electronics Division, The Electrochemical Society, (1969).
2. C. Y. Chang and S. M. Sze, *Solid-St. Electron.* **13**, 727 (1970).
3. F. A. Padovani and R. Stratton, *Solid-St. Electron.* **9**, 695 (1966).
4. C. R. Crowell and V. L. Rideout, *Solid-St. Electron.* **12**, 89 (1969).
5. C. R. Crowell, *Solid-St. Electron.* **8**, 395 (1965); and *Solid-St. Electron.* **12**, 55 (1969).
6. H. D. Barber, *Solid-St. Electron.*, **10**, 1039 (1967).
7. S. M. Sze, C. R. Crowell and D. Kahng, *J. appl. Phys.* **35**, 2534 (1964).
8. R. A. Stradling and V. V. Zhukov, *Proc. Phys. Soc. London* **87**, 263 (1966).
9. M. Neuberger, *GaAs—A Bibliography Supplement*, DS-144 (Supplement No. 4), Electronic Properties Information Center, Hughes Aircraft Co., Culver City, California, December (1969).
10. J. Vilms and L. Wandinger, Theory of contact resistance for one type of ohmic contact. A chapter In *Ohmic Contacts to Semiconductors* Electronics division, The Electrochemical Society, Inc. (1969).
11. C. R. Crowell and S. M. Sze, *Solid-St. Electron.* **8**, 979 (1965).